Electronic structure of $CoSi_2$ films on Si(111) studied using time-resolved two-photon photoemission

2009 J. Phys.: Condens. Matter 21 134006

(http://iopscience.iop.org/0953-8984/21/13/134006)

J. Phys.: Condens. Matter **21** (2009) 134006 (9pp) doi:10.1088/0953-8984/21/13/134006

Electronic structure of $CoSi_2$ films on Si(111) studied using time-resolved two-photon photoemission

M Kutschera[1], T Groth[1], C Kentsch[1], I L Shumay[1], M Weinelt[2] and Th Fauster[1]

[1] Lehrstuhl für Festkörperphysik, Universität Erlangen-Nürnberg, Staudtstraße 7, 91058 Erlangen, Germany
[2] Max-Born-Institut, Max-Born-Straße 2A, 12489 Berlin, Germany

E-mail: fauster@physik.uni-erlangen.de

Received 7 November 2008
Published 12 March 2009
Online at stacks.iop.org/JPhysCM/21/134006

Abstract

The occupied and unoccupied electronic structure of thin epitaxial $CoSi_2$ films grown on Si(111) substrates was studied using time-resolved two-photon photoemission and valence-band photoemission spectroscopy. The work function of the sample surfaces and the Schottky barrier height at the metal–semiconductor interface were measured as a function of annealing temperature. The photoemission data reveal several occupied and unoccupied electronic states which exhibit a high sensitivity to the annealing temperature. Time-resolved measurements show a behavior typical for a short-lived hot-electron gas and indications for an image-potential resonance.

1. Introduction

Transition metals either as pure films or as silicide compounds, both on top of silicon, are widely used and play an important role in silicon-based devices [1, 2]. On one hand they act as metallic interconnections and ohmic contacts. On the other hand they also form very good Schottky contacts which are preferred in the field of optoelectronics. Cobalt disilicide films show some outstanding features which make this material not only a proper candidate in technology but also one in fundamental research. $CoSi_2$ has a small lattice mismatch of -1.2% with respect to silicon and it develops an atomically sharp interface without intermixing with the underlying silicon even at elevated temperatures rendering it compatible with microchip processing. In addition, $CoSi_2$ is a good conduction metal with all the above-mentioned possible applications in technology. In particular $CoSi_2$ films grown on (111)-oriented substrates present near-perfect crystalline order with very few defects [3].

The growth mechanism and the geometric structure have been extensively studied before [4–9]. After deposition of 3–10 monolayers (ML) of cobalt and annealing to 300–460 °C a cobalt-rich phase ($CoSi_2$-C) forms. It shows a 1×1 low-energy electron diffraction (LEED) pattern and corresponds to a bulk-terminated cobalt disilicide surface [9]. It consists of Si–Co–Si trilayers separated by 3.10 Å with an intralayer distance of 0.77 Å. Further annealing to 500–650 °C leads to a silicon-rich phase ($CoSi_2$-S) which has an additional bilayer of silicon on top. For the usually observed 2×1 or 2×2 reconstruction no quantitative structural model exists. At even higher annealing temperatures pinholes form and the 7×7 reconstruction of the Si(111) substrate appears [10].

The occupied part of the electronic band structure of $CoSi_2$ films has been investigated using angle-resolved photoemission [9, 11–14]. Besides surface states, also quantum-well states were found as standing waves in thin films, sampling the bulk band structure of $CoSi_2$ [15, 16]. Ballistic electron emission microscopy (BEEM) yielded some information on the unoccupied part of the band structure [17] which might be important for the performance of hot-electron devices.

We investigated the electronic structure of the $CoSi_2$ surface using time-resolved two-photon photoemission (2PPE). The unoccupied states are excited from occupied states by a first photon and emitted by a second photon as illustrated at the left in figure 1. Two-photon photoemission brings the high-energy resolution and high sensitivity of photoelectron spectroscopy to the unoccupied states. In

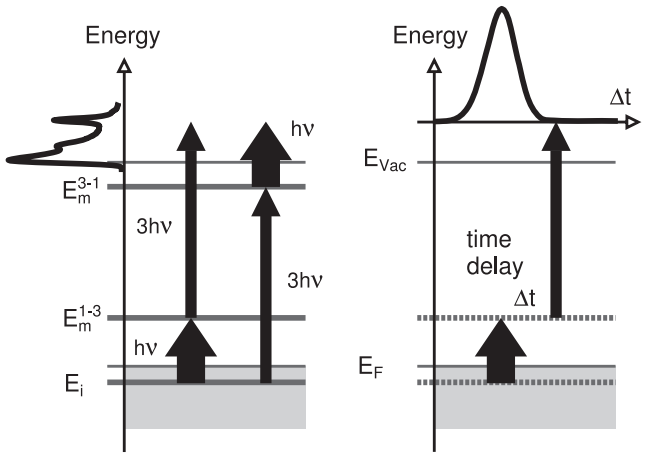

Figure 1. Energy diagram of two-photon photoemission showing two different excitation processes in energy-resolved spectroscopy at the left and the time-resolved mode at the right.

addition, information on the work function of the surfaces and the band alignment at the metal–semiconductor interface (Schottky barrier height) is obtained [18]. Two-photon photoemission accesses the occupied states as well and we performed regular photoemission for direct comparison. The time-resolved mode (figure 1, right) samples directly the electron dynamics and gives information about the decay of hot electrons.

2. Experiment

Silicon substrates were cut from p-doped (boron, 1–10 Ω cm) (111)-oriented wafers. The initial preparation consisted of a careful removing of organic contaminants with acetone and methanol followed by rinsing in distilled water which was in turn blown off with compressed air. The substrates were then mounted on the sample holder and the ultra-high-vacuum chamber was baked. After the chamber reached its base pressure of 5×10^{-11} mbar the sample was outgassed by direct resistive heating at 500 °C for at least 2 h. The substrate preparation was then done by flashing to 1200 °C for a few seconds, carefully watching that the chamber pressure does not rise above 5×10^{-10} mbar, followed by a slow cooling down from 900 °C to room temperature (RT) at a rate of about 1 °C s^{-1}. As a result a very sharp 7 × 7 LEED pattern with nearly no background intensity was obtained. Subsequent preparations were done by sputter cleaning for about 2 h to remove $CoSi_2$ films, followed by the above described flashing and cooling procedure. No change in substrate and film quality could be observed even after about 20 preparation cycles when substrates were changed.

Cobalt was evaporated *in situ* from an electron-beam heated source with built-in flux monitor onto the 7 × 7-reconstructed Si(111) held at room temperature. The desired amount of cobalt (in ML of the $CoSi_2$(111) structure) was calibrated immediately before each deposition by means of a quartz microbalance which was put in the same position as the sample. Cobalt films were then annealed to the desired reaction temperature for 3 min and quenched immediately down to the measurement temperature of −150 °C. Special attention was paid to controlling the sample temperature within ±10 °C while heating. This was done with a W–Re thermocouple pressing on the back of the sample and an infrared pyrometer which was able to measure temperatures between 300 and 1400 °C.

For the 2PPE experiments a Ti:sapphire laser system was used which produced ultra-short pulses with 45 fs duration as fundamental radiation ($h\nu$) and frequency-tripled pulses ($3h\nu$) with 75 fs duration [19, 20]. Besides this bichromatic mode some experiments were done using $3h\nu$ photons only (monochromatic mode). Observed peaks are denoted in this work with subscripts 1 and 2 for monochromatic and bichromatic 2PPE and U for UPS, respectively. The laser pulses were hitting the sample surface at an incidence angle of 45° perpendicular to the [1$\bar{1}$0] axis of the mirror plane. Electrons emitted within a cone of 0.6° opening angle around the surface normal were then detected by means of a hemispherical energy analyzer with ≈45 meV energy resolution. Ultraviolet photoemission spectroscopy (UPS) was performed using He I radiation at 21.2 eV photon energy from a rare-gas discharge lamp.

3. Temperature dependence

3.1. Two-photon photoemission

To monitor the formation of $CoSi_2$ from the deposited cobalt and the evolution of the aforementioned film phases, 2PPE spectra were recorded for different annealing temperatures (figure 2). The observed LEED patterns for this annealing sequence are indicated at the right. The cobalt film shows before annealing a diffuse LEED pattern and a rather featureless 2PPE spectrum indicating a poorly ordered $CoSi_2$ film. Mild annealing is sufficient to start the silicide reaction. The first indications of the $CoSi_2$-C-phase can be seen at −0.5 eV for annealing temperatures of ∼200 °C where no clear LEED pattern is visible yet. This C_2 feature is best developed at 350 °C annealing temperature when the 1 × 1 LEED pattern indicates the well-ordered C-phase. At higher annealing temperatures of about 450 °C the LEED pattern shows fractional diffraction spots. The observed change in the intensity of the integer-order LEED reflexes indicates the transition from C- to S-phase [8, 21]. The S-phase shows two prominent features (A_2, E_2) in the 2PPE spectra recorded at 1.54 eV photon energy. The silicon-rich phase proved to be stable up to 650 °C. At higher annealing temperatures the 2PPE peaks slowly degraded and vanished.

3.2. Work function and Schottky barrier height

The low-energy cutoffs in figure 2 show a variation with temperature which can be related directly to the work function Φ of the $CoSi_2$ films via the width of the spectra $h\nu_{tot} - \Phi$. The total photon energy $h\nu_{tot}$ is $4h\nu$ for the bichromatic 2PPE spectra. The results for films in the thickness range of 3–10 ML Co are shown in figure 3 by open symbols (circles from 2PPE and squares from UPS spectra, respectively). From the

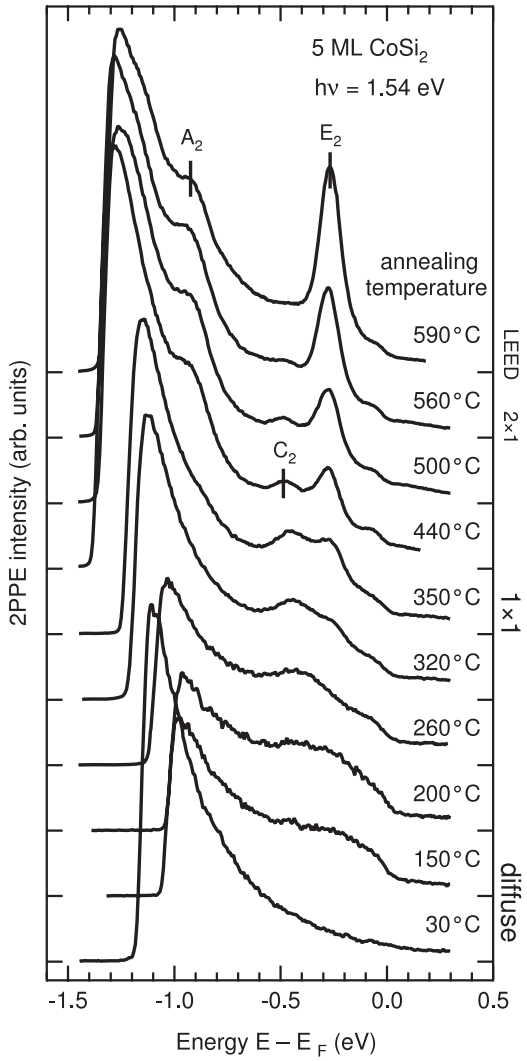

Figure 2. Bichromatic two-photon photoemission spectra ($h\nu = 1.54$ eV) from a 5 ML cobalt film deposited on Si(111) at RT and annealed to the indicated temperatures. The energy scale indicates the initial-state energy of the 2PPE transition relative to Fermi energy E_F. The observed LEED patterns are indicated at the right.

plateaus in the temperature range of the C- and S-phase we obtain the work functions as 5.15±0.05 eV and 4.82±0.05 eV, respectively. This trend in lowering the work function during annealing of the films has been reported before [21, 22]. It is attributed to surface segregation of a double layer of silicon. The literature values measured at lower-energy resolution are about 0.15 eV smaller (4.95 and 4.70 eV) than the data obtained in this work.

Two-photon photoemission permits a direct spectroscopic determination of the Schottky barrier height. At low temperatures, high photon intensities lead to a saturation of the photovoltage, which is in this case the difference between the Fermi levels in the metal and the semiconductor [18]. The results for films with thickness <10 ML are shown in figure 3 by filled symbols. The Schottky barrier height varies between 0.4 and 0.6 eV depending on the annealing temperature. This variation is reduced for thicker films (>10 ML) which proves

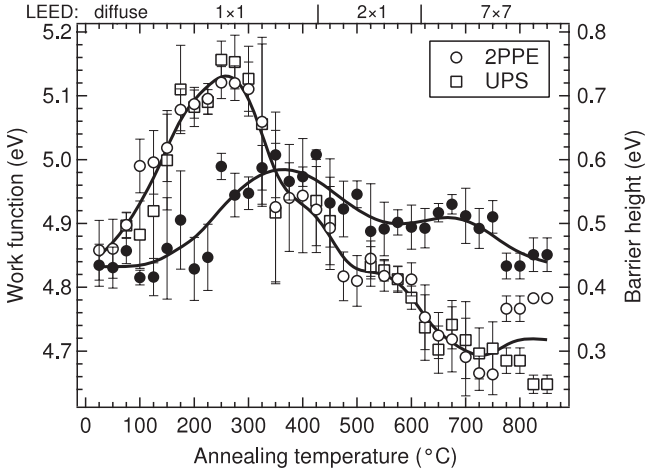

Figure 3. Work function (open symbols, left scale) and Schottky barrier height (filled symbols, right scale) of $CoSi_2$ films (3–10 ML) on Si(111) as a function of annealing temperature. The error bars indicate the observed range of values for different sample preparations. The observed LEED patterns are indicated at the top of the graph.

that the Schottky barrier height is an interface property. As evident from the uncorrelated temperature dependence of the work function and barrier height in figure 3, the Schottky barrier is not solely determined by the work function difference between the Si substrate and $CoSi_2$ film. The barrier must contain significant contributions from interface states, which vary with the annealing temperature. In contrast, the work function as a surface property shows a much larger variation with temperature as seen in figure 3.

Our data for the Schottky barrier height of 0.40–0.43 eV at room temperature and 0.51 eV (0.43 eV for thicker films) after annealing to 650° agree with values reported in the literature, of 0.43 eV [23] and 0.47 eV [23] or 0.50 eV [24], respectively.

4. Electronic states of the cobalt-rich C-phase

The spectra in figure 4 were measured for 5 ML cobalt annealed to 500 °C. The temperature was chosen to be in the intermediate region so both the peaks of the C- and those of the S-phase are visible. The UPS spectrum (dots and thin curve) shows several peaks. The Λ_3 and Λ_1 (not shown) bulk states as well as the S1 (C-phase, not shown) and S2 (S-phase) surface states are observed with improved energy resolution at the same binding energies (±0.05 eV) as in previous work [16]. Additionally a series of 3–5 peaks with binding energies below 0.8 eV were clearly visible. The dependence of the observed energetic position on the film thickness has led to the assignment to quantum-well states within the $CoSi_2$ film [15, 16, 25]. This is supported by the observation of these states at similar energies for annealing temperatures of 460 and 560 °C.

Stadler *et al* [26] calculated surface states at $\overline{\Gamma}$ for the C-phase at −1.5, −3.0, and −3.7 eV below E_F. The observed energies are −1.5 eV (Λ_3), −2.0 eV (Λ_1), and −2.75 eV (S1 surface state) and were assigned by Haderbache *et al* as direct transitions using a free-electron final state [15, 16, 25].

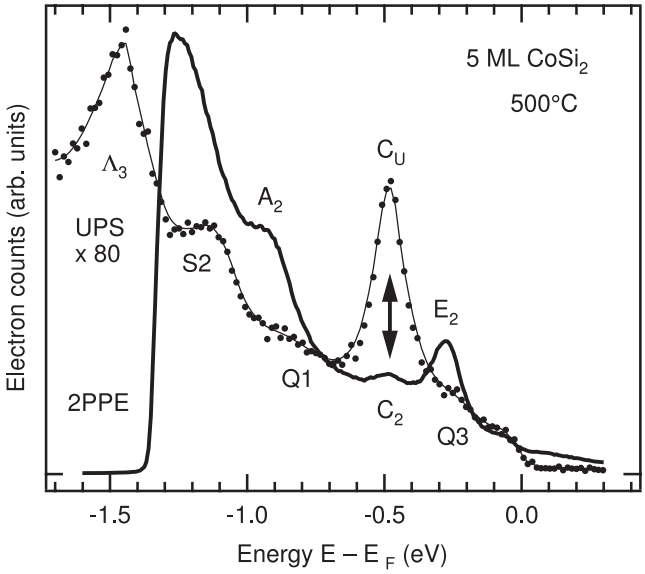

Figure 4. Comparison of a valence-band spectrum (UPS, $h\nu = 21.2$ eV) with a bichromatic two-photon photoemission spectrum at normal emission ($h\nu = 1.54$ eV) from a 5 ML cobalt film annealed to 500 °C. The similarity in energy and dependence on annealing temperature (not shown) of peaks C_2 (2PPE) and C_U (UPS) supports an interpretation as an initial state.

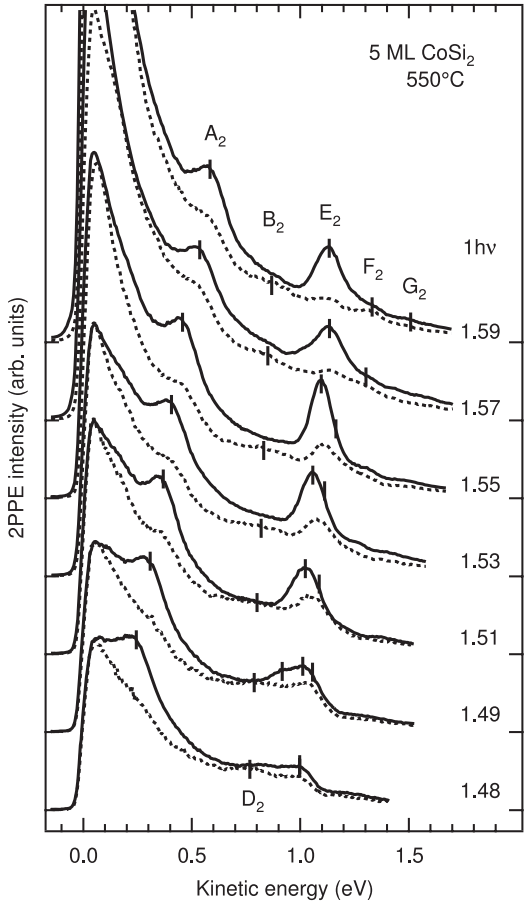

Figure 5. Bichromatic two-photon photoemission spectra for different photon energies $h\nu$ at normal emission from a 5 ML cobalt film on Si(111) annealed to 550 °C. Solid and dashed lines are for p- and s-polarized frequency-tripled ($3h\nu$) light, respectively. The fundamental ($h\nu$) beam is always p-polarized.

The bichromatic 2PPE spectrum in figure 4 (solid line) is shown for comparison to the UPS data taken for the same sample. The most striking result is the identical energetic position at −0.50 eV of peak C_2 and C_U from the 2PPE and the UPS spectra, respectively. Furthermore these peaks develop and vanish at the same annealing temperature. Therefore, peaks $C_{U/2}$ are assigned to photoemission from an occupied initial state. It is interesting to note that this peak is observed only for coverages up to 5 ML which makes an assignment to a surface state unlikely. A possible explanation could be an interface state near the valence-band maximum of silicon. Its existence might be intrinsically related to the Schottky barrier height. This could explain why this state is not observed for thicker films and for the S-phase.

5. Electronic states of the silicon-rich S-phase

5.1. Two-photon photoemission results

Figure 5 shows bichromatic 2PPE spectra of a 5 ML cobalt film annealed to 550 °C to form $CoSi_2$-S. The spectra were recorded using photon energies $h\nu$ ranging from 1.48 to 1.59 eV. Three different combinations of the polarization of the $h\nu$ and $3h\nu$ light pulses were used in the experiment: p/p, p/s and s/p (spectra not shown in figure 5). The peaks A_2 and E_2 typical for the $CoSi_2$-S-phase were already identified in figure 2 and can be observed at all photon energies. The changing shape at higher kinetic energies in the spectra reveals further transitions (B_2, D_2, F_2 and G_2) which cannot be clearly resolved in the p/p spectra due to the high intensity of peak E_2. Using s-polarized $3h\nu$ light the intensity of peaks A_2 and E_2 is suppressed (dashed lines in figure 5) whereas peaks B_2, D_2 and F_2 show increased count rate compared to the background. Peak G_2 appears as a rather faint feature close to the Fermi edge and cannot be followed over the entire photon energy range. The same holds for peaks D_2 and F_2 which are only visible at low and high photon energies respectively. Neither peak B_2 nor peak D_2 is identical with peak C_2 of the C-phase at lower temperatures.

The monochromatic 2PPE spectra shown in figure 6 for photon energies from $3h\nu = 4.43$ to 4.74 eV are recorded using p-polarized $3h\nu$ light. Due to the larger energy range accessible a total of 11 peaks can be identified with varying photon energy. Peaks A_1 and F_1 seem to be identical to their bichromatic counterparts (A_2 and F_2).

All peaks in the monochromatic and bichromatic 2PPE spectra are visible over a sufficiently large range of photon energies. Their energy positions were fitted using a Lorentzian plus an exponentially decaying background convoluted with a Gaussian distribution representing the experimental resolution. The resulting peak positions are plotted in figure 7 as a function of photon energy. Data from monochromatic 2PPE spectra are shown with filled symbols and those from bichromatic experiments with open symbols. Points extracted from spectra with s- and p-polarized $3h\nu$ light are represented by squares and circles, respectively. All peaks observed show a linear dependence on photon energy. The fitted slopes α =

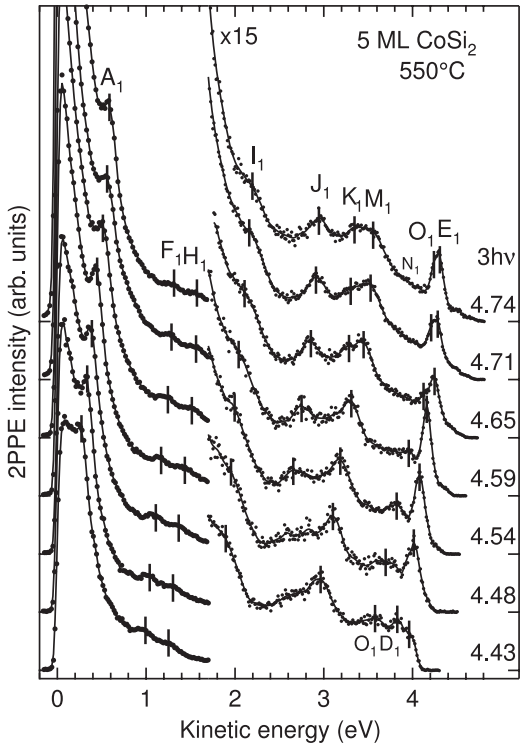

Figure 6. Monochromatic two-photon photoemission spectra ($3h\nu$ light only) at normal emission from a 5 ML cobalt film on Si(111) annealed to 550 °C for different photon energies. At kinetic energies above 1.7 eV the 2PPE intensity is multiplied by a factor of 15.

$\Delta E_{\mathrm{kin}}/\Delta h\nu$ are listed in table 1. Values with a rather high uncertainty due to a limited number of data points are given in parentheses. In table 1 the energies for the initial ($E_{\mathrm{i}} = E_{\mathrm{kin}} - h\nu_{\mathrm{tot}} + \Phi$) and possible intermediate ($E_{\mathrm{m}}^{1-3} = E_{\mathrm{i}} + h\nu$, $E_{\mathrm{m}}^{3-1} = E_{\mathrm{m}}^{3-3} = E_{\mathrm{i}} + 3h\nu$) states are given relative to the Fermi energy E_{F} for a photon energy of $h\nu = 1.52$ eV. The last columns for the bichromatic spectra show for which polarization of the laser light the peak was observed. Underlined values mark transitions observed in monochromatic 2PPE which should also be accessible in bichromatic spectra.

Surface or quantum-well states have a well-defined energy in contrast to dispersing bulk bands. The observed kinetic energy depends on the number of photons absorbed in the photoemission process. For unoccupied intermediate states either a photon of energy $h\nu$ or one of energy $3h\nu$ leads to emission, resulting in slope $\alpha = 1$ or $\alpha = 3$, respectively. For monochromatic 2PPE only the latter value is possible. For occupied initial states the slope is $\alpha = 4$ in bichromatic 2PPE and $\alpha = 6$ for monochromatic 2PPE.

All transitions listed in table 1 have slopes consistent with these considerations and may be assigned to surface or quantum-well states. The assignment of the transition to an initial or intermediate electronic state according to the observed slope is indicated by energy values printed in bold. A comparison shows that the peaks $\mathsf{A}_{1/2}$, $\mathsf{D}_{1/2}$, $\mathsf{E}_{1/2}$ and $\mathsf{F}_{1/2}$ are related to the same electronic states probed with monochromatic and bichromatic 2PPE spectroscopy, respectively.

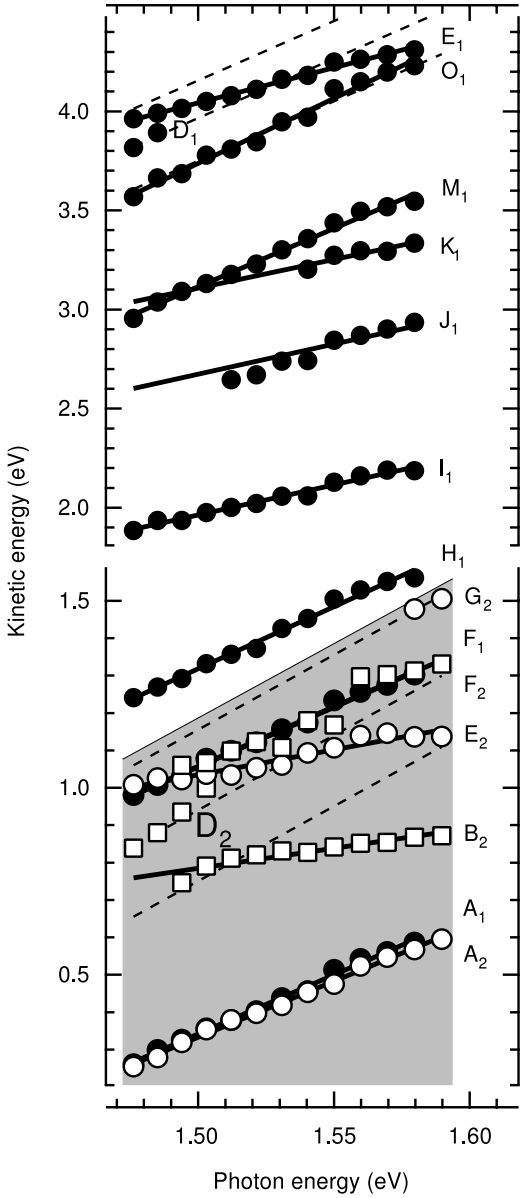

Figure 7. Kinetic energies of the peaks in the 2PPE spectra as a function of photon energy. Open and filled symbols are from bichromatic (figure 5) and monochromatic (figure 6) 2PPE spectra. Peaks better seen with s-polarized $3h\nu$ light (bichromatic spectra) are indicated by squares instead of circles. The shaded area indicates the energy range accessible with bichromatic 2PPE spectroscopy. Note the expanded kinetic energy scale in the lower part of the diagram.

5.2. Assignment of transitions

For the interpretation of the experimental 2PPE results the knowledge of the bulk band structure is important [28]. In addition it permits the identification of gaps in the projected bulk band structure where surface states may exist. For thin films investigated here quantum-well states derived from bulk bands might form. Figure 8 shows a band structure calculation for bulk $CoSi_2$ [27] (similar to [29–31]). Totally symmetric bands of Λ_1 symmetry are shown as solid lines, whereas dashed curves represent bands of Λ_3 symmetry. This information is relevant for the identification of symmetry

Table 1. Experimentally observed 2PPE transitions in the bichromatic and monochromatic two-photon photoemission spectra at a photon energy of $h\nu = 1.52$ eV. The slope α is the ratio of the change of kinetic energy to the change of photon energy $h\nu$. Bold values indicate the assignment to an initial or an intermediate state according to the slope α. The light polarization needed to observe the transitions is given for the data from bichromatic 2PPE. The underlined transitions should energetically also be visible in the bichromatic spectra. At the lower right part the observed UPS initial states are given for comparison. All energies are given in eV relative to E_F.

Bichromatic 2PPE							
Peak	α	E_i	E_m^{1-3}	E_m^{3-1}	Pol. ($h\nu/3h\nu$)		
A_2	3.0	−0.88	**0.65**	3.69	p/p		s/p
B_2	1.1	−0.46	1.06	**4.10**		p/s	
D_2	(4)	**−0.24**	1.28	4.32	p/p	p/s	
E_2	1.3	−0.21	1.31	**4.36**	p/p		
F_2	3.2	−0.15	**1.38**	4.42		p/s	s/p
G_2	(4)	**−0.03**	1.49	4.53	p/p	p/s	

Monochromatic 2PPE				UPS	
Peak	α	E_i	E_m^{3-3}	Peak	E_i
A_1	3.2	−3.92	**0.65**		
F_1	3.2	−3.20	**1.37**		
H_1	3.3	−2.94	**1.63**		
I_1	3.0	−2.30	**2.27**		
J_1	(3)	−1.59	**2.98**		
				Λ_3	**−1.46**
K_1	2.9	−1.16	**3.41**		
M_1	5.9	**−1.08**	3.48	S2	**−1.08**
N_1				Q1	**−0.82**
O_1	6.5	**−0.45**	4.12	Q2	**−0.45**
D_1	(6)	**−0.23**	4.34	Q3	**−0.22**
E_1	3.6	−0.21	**4.36**		

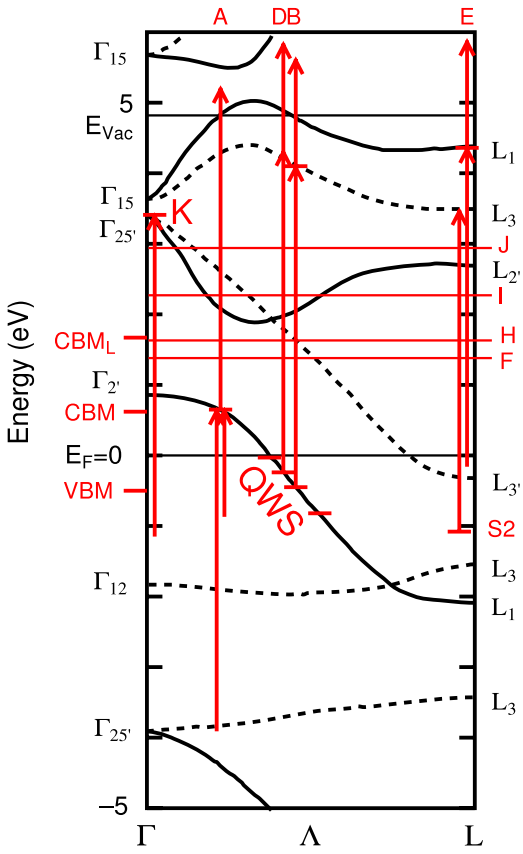

Figure 8. Band structure of bulk $CoSi_2$ along the Λ axis ΓL taken from [27]. Bands of Λ_1 and Λ_3 symmetry are shown by solid and dashed lines, respectively. Experimentally observed transitions and states involved are indicated by arrows and short lines.

(This figure is in colour only in the electronic version)

gaps and the interpretation of the polarization dependence. An available calculation of the surface electronic structure of 2 × 1 terminated $CoSi_2$ [32] relies on a hypothetical surface geometry and cannot reproduce the results from our measurements.

5.2.1. Band gaps and quantum-well states. The band structure calculation of figure 8 shows an absolute band gap only for the occupied states between −3.4 and −2.2 eV. For the existence of surface states of a particular symmetry a band gap for the bands of the same symmetry is sufficient. This consideration would allow Λ_1 surface states in the energy range between −3.9 and −2.2 eV as well as between 0.8 and 1.8 eV. The energy gap around 3.5 eV is rather narrow and the distinction between surface and bulk states might be difficult. Surface states of Λ_3 symmetry could exist between −3.4 and −2.0 eV as well as between −1.6 and −0.3 eV. The 2 × 1 reconstruction folds back states from the $\overline{M}$ point of the unreconstructed surface Brillouin zone (LX line) to the $\overline{\Gamma}$ point. This backfolding closes all band gaps [32, 33]. Depending on the strength of the backfolding, the band gaps of the unreconstructed surface might still be relevant for the existence of surface states which should correctly then be called surface resonances.

For the surface of a $CoSi_2$ crystal the number of surface states cannot exceed the number of band gaps at the center of the surface Brillouin zone [34]. The number of observed surface states (slope $\alpha = 1, 3, 4$, or 6 in table 1) is much larger than the number of band gaps. Therefore some of the peaks have to be assigned to quantum-well states which are confined to the overlayer or image-potential states located in the vacuum region. Quantum-well states are found in energy ranges where overlayer bands exist and the substrate has no states of matching symmetry. From the measured Schottky barrier height we locate the valence-band maximum at −0.51 eV below the Fermi energy of the $CoSi_2$ film. The absolute conduction-band minimum is then located at 0.65 eV above E_F. Along the (111) direction the band minimum has an energy of 1.7 eV. This minimum is of Λ_1 symmetry, so quantum-well states could form in the Λ_1 band of $CoSi_2$ for all energies above the Si valence-band maximum. For Λ_3 states the conduction band with the lowest energy starts at 2.9 eV. Quantum-well states of Λ_3 symmetry could therefore be derived from the Λ_3 band crossing E_F almost up to the band maximum. In principle, the 2 × 1 reconstruction could lead to quantum-well states along the LX line of the bulk band structure. Because of the considerable parallel momentum of the electrons in the $CoSi_2$ layer, we do not consider this possibility any further.

5.2.2. Dipole selection rules. The dipole selection rules for normal emission along the (111) direction (Λ axis) of the fcc-based $CoSi_2$ structure are particularly simple [35]. A component of the field vector parallel to the (111) direction couples only states of the same symmetry. A component perpendicular to the (111) direction permits transitions between Λ_3 states and all other symmetry representations. This situation occurs for s-polarized light. However, p-polarized light at an angle of incidence of 45° relative to the (111) direction has electric field components parallel as well as perpendicular to the Λ axis. Note that the selection rules are independent of the azimuthal orientation of the sample. For the symmetry assignment of the observed states one should keep in mind that the final state has to be totally symmetric (Λ_1) and that only bands of Λ_1 and Λ_3 symmetry exist in the relevant energy range (see figure 8). Lacking information on the symmetry of the bands along the LX line [30] we cannot establish dipole selection rules for the backfolded bands.

5.2.3. Occupied surface and quantum-well states. The assigned states and observed transitions from table 1 are marked by lines and indicated by arrows in the bulk band structure of figure 8.

The surface state S2 is observed in monochromatic 2PPE as peak M_1. According to the bulk band structure the state lies in the L_3–$L_{3'}$ band gap. The 2PPE transition occurs via the next L_3 point and the intensity seems to decrease towards the edges of the photon energy range shown in figure 6. The high background near the low-energy cutoff might explain why the corresponding peak cannot be seen in the bichromatic 2PPE mode.

The occupied quantum-well states Q observed in UPS are also seen in 2PPE spectra as peaks N_1, O_1, $D_{1/2}$, and G_2. The intensity is rather weak, independently of the exciting photons and significantly lower than for the surface state S2. The separation in the $k_\perp$ direction along the Λ_1 band seems rather small for a 5 ML film and the energies of the peaks do not show the expected strong thickness dependence. A possible cause could be the coexistence of several layer thicknesses. However, the observed peaks exhibit a rather narrow linewidth, so the superposition of quantum-well states for different thicknesses seems unlikely. The energy of the lowest quantum-well state is below the valence-band maximum of silicon. However, quantum-well states outside the band gap have been observed for Pb on Si(111) [36].

5.2.4. Unoccupied states. Peaks $A_{1/2}$ are assigned to an intermediate state 0.65 eV above the Fermi level. The bulk band structure (figure 8) shows no energy gap at this energy excluding the assignment as a surface state. Photoemission from the unoccupied Λ_1 band near or at the $\Gamma_{2'}$ point seems a satisfactory explanation. This classification also accounts for the fact that p-polarized light is needed for the ionization step. In monochromatic 2PPE the initial state could be close to the $\Gamma_{25'}$ point, whereas no initial state seems to be available in bichromatic 2PPE. The free-electron-like band starting at the Γ_{15} point provides the final state. In thin films the bulk bands should show quantum-well behavior. No significant shift with

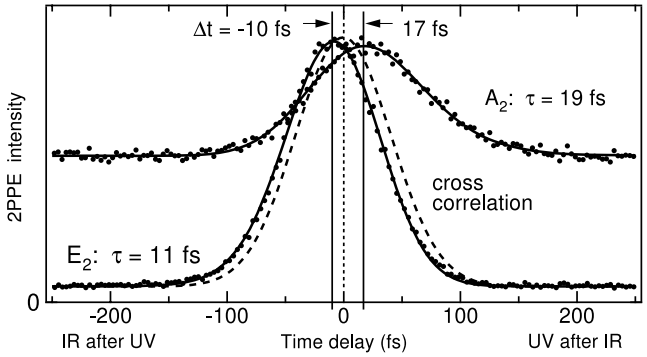

Figure 9. Time-resolved two-photon photoemission traces for peaks A_2 and E_2. The dashed line shows the cross-correlation of the laser pulses for the determination of zero time delay.

film thickness has been observed for peaks $A_{1/2}$, in agreement with calculations [17]. The experimental results from ballistic electron emission microscopy [17] at slightly larger film thicknesses show similar energies but a stronger dependence on film thickness. It should be noted that the energy of peaks $A_{1/2}$ coincides with the conduction-band minimum of the silicon substrate. So emission of photoexcited conduction-band electrons through the silicide layer is possible. The filling time at the band bottom is a few hundred fs to 1 ps [36, 37]. The lifetime of A_2 is much shorter and no slowly decaying component is observed (see figure 9), which makes an assignment to the conduction-band minimum of Si very unlikely. It should be noted that at the excitation densities used in this work and previous work on Si(100) [18, 38, 39] we have never seen significant contributions from the conduction-band minimum of Si(100), in contrast to the case for measurements at higher excitation densities [36, 37].

Peaks $E_{1/2}$ show relatively high intensity in the spectra (see figures 5, 6) at an intermediate-state energy of 4.36 eV. According to the band structure an assignment to the flat part of the Λ_1 band near the L_1 point seems plausible. The observation with p-polarized light in the second excitation step agrees with this assignment. No initial state can be identified in figure 8. The relatively long lifetime of the intermediate state E_2 (see section 5.3) explains the strong intensity of the peak. This suggests an interpretation as an image-potential resonance with a binding energy relative to the vacuum level of 0.46 eV similar to the value found for on Si(100) [40]. Adsorption of 27 L (langmuirs) of oxygen increases the work function by 0.3 eV. However, the energy of peak E_2 stays constant relative to E_F. For an image-potential resonance the energy should show a similar shift as the vacuum level. A possible explanation could be a strong coupling of the image-potential resonance to the $CoSi_2$ quantum well which pins the energy to the Λ_1 band [41].

The remaining peaks show relatively low intensity compared to the unoccupied states discussed so far. Peaks $F_{1/2}$ are observed using both 2PPE methods as an unoccupied intermediate state 1.38 eV above E_F. The observed slope is not compatible with the strongly dispersing Λ_3 bulk band located in this energy range. The polarization analysis does not permit a unique assignment of the symmetry of the state and no clear assignment of initial states is possible. A possible

interpretation would be a surface or quantum-well state lying in the symmetry gap of the Λ_1 states. A quantum-well state derived from the Λ_3 band was observed in BEEM [17].

For peak H_1 no clear assignment comes from the bulk band structure like for the case of transition $F_{1/2}$. The energy would match the X_3 point backfolded by the 2×1 reconstruction. The energies of the intermediate states associated with peaks I_1 and J_1 match two strongly dispersing bulk bands which is at variance with the observed slope.

Peak K_1 is found at the same energy as the $\Gamma_{25'}$ point. However, no matching initial band is available. A surface state in the small gap between the $\Gamma_{25'}$ and Γ_{15} points is an alternate interpretation.

Peak B_2 is only distinguishable from the background intensity in bichromatic 2PPE spectra when using s-polarized $3h\nu$ light to pump electrons into the unoccupied state at 4.1 eV above the Fermi energy. A possible interpretation could be a process where electrons are excited from an occupied quantum-well state in the Λ_1 bulk band into the Λ_3 band.

5.3. Lifetimes

The lifetime of intermediate states was measured directly by varying the time delay between pump and probe pulse. The time-resolved spectra recorded at the energies of the A_2 and E_2 states are shown as functions of time delay Δt in figure 9. The cross-correlation (dashed curve) between the UV ($3h\nu$) and IR ($h\nu$) laser pulses was measured on the occupied surface state of a Cu(111) reference sample [42] mounted on the same sample holder. The time-resolved spectra are shifted relative to $\Delta t = 0$. For the peak A_2 the shift indicates that the UV pulse comes after the IR pulse. The opposite excitation sequence applies to peak E_2. This confirms the results derived from the photon energy dependence of figure 7 and table 1. The shift of the maximum intensity is a good estimate for lifetimes shorter than the cross-correlation width of 95 fs [42, 43]. The more detailed fits give for the intermediate state A_2 a lifetime of 16 ± 9 fs which is significantly higher than for the background at nearby energies. The lifetime of state E_2 was determined as 10 ± 6 fs. This value is rather high for a state lying 4.36 eV above E_F in a metallic film. From the energetic position relative to the vacuum level an interpretation as an image-potential resonance seems plausible. For these states the overlap with bulk states is rather small, leading to long lifetimes [42, 44].

The 2PPE spectrum in figure 10 (dot–dashed curve) shows besides the peaks discussed a considerable background which permits the determination of lifetimes. These are attributed to the lifetimes of excited electrons. A simple interpretation within a free-electron-gas model predicts a $\gamma(E - E_F)^{-2}$ dependence as indicated by the solid line in figure 10. The prefactor of $\gamma = 2.2$ fs is comparable to values found for ferromagnetic surfaces [45]. The density of states of $CoSi_2$ [27, 29] shows a strong peak below E_F related to Co 3d states, similar to the case for the ferromagnets. Mean free paths of excited electrons measured using BEEM [46] have been found in agreement with thickness-dependent photoyield measurements [47]. The short-dashed line shows these results [46] converted to lifetimes using an electron velocity of 9.5 Å fs^{-1} [27]. This evaluation yields values slightly larger than our results.

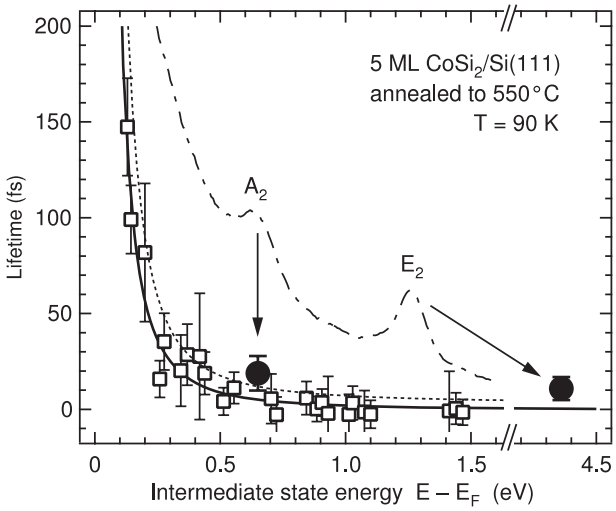

Figure 10. Lifetime of the hot electrons in the $CoSi_2$ film and lifetime of excited electrons in the intermediate states measured with time-resolved two-photon photoemission. The dot–dashed line shows the 2PPE spectrum for identification of the peaks.

6. Summary and conclusions

The occupied as well as the unoccupied part of the electronic band structure of $CoSi_2$ films grown on Si(111) substrates was studied using two-photon photoemission and valence-band spectroscopy. The cobalt-rich and silicon-rich surfaces ($CoSi_2$-C and $CoSi_2$-S) were prepared by appropriate annealing for thicknesses up to 20 ML. The sample preparation was monitored using LEED and photoelectron spectra. The work function and Schottky barrier height as functions of annealing temperature were determined with higher accuracy, in reasonable agreement with previous results [21–24]. Many occupied and unoccupied states were found in the 2PPE spectra and the experimental results are assigned to transitions involving quantum-well states, surface states and an image-potential resonance. For two unoccupied states the lifetime was determined using time-resolved 2PPE. The lifetime of hot electrons in $CoSi_2$ is comparable to that of ferromagnetic surfaces.

The interpretation of the results in relation to available band structure calculations of $CoSi_2$ is only partially successful for the following reasons. (i) The information on backfolded bands for the reconstructed surface is limited. (ii) The geometric structure of the reconstructed surface is not known. Therefore no reliable calculation of surface states exists. (iii) The coupling between initial and intermediate states in 2PPE can be used to obtain information on the bulk band structure [28]. It is not clear how these considerations affect the study of quantum-well states. The limited success in comparing experimental results with band structure calculations for $CoSi_2$ layers on Si(111) is not surprising considering the complexity of the system. For the clean Si(100) surface not all observed 2PPE transitions could be interpreted unambiguously [39]. The agreement between 2PPE results on Si(557)–Au and a calculated surface band structure is also rather poor [48]. Obviously more effort is needed

for a complete understanding of 2PPE and its relation to the electronic structure for complex surfaces.

Acknowledgments

We enjoyed many stimulating discussions with Klaus Heinz and acknowledge the advice of Ulrich Starke on the sample preparation. This work has been supported in part by Deutsche Forschungsgemeinschaft through Sonderforschungsbereich 292.

References

[1] Murarka S P 1995 *Intermetallics* **3** 173
[2] Tung R T and Ohmi S 2000 *Thin Solid Films* **369** 233
[3] Derrien J and Arnaud d'Avitaya F 1987 *J. Vac. Sci. Technol.* A **5** 2111
[4] Seubert A, Schardt J, Weiß W, Starke U, Heinz K and Fauster T 2000 *Appl. Phys. Lett.* **76** 727
[5] Starke U, Schardt J, Weiß W, Rangelov G, Fauster T and Heinz K 1998 *Surf. Rev. Lett.* **5** 139
[6] Ilge B, Palasantzas G, de Nijs J and Geerligs L J 1998 *Surf. Sci.* **414** 279
[7] Stalder R, Sirringhaus H, Onda N and von Känel H 1991 *Surf. Sci.* **258** 153
[8] Hellman F and Tung R T 1988 *Phys. Rev.* B **37** 10786
[9] Rangelov G, Augustin P, Stober J and Fauster T 1994 *Surf. Sci.* **307** 264
[10] Tung R T 1992 *Mater. Chem. Phys.* **32** 107
[11] Pirri C, Hong S, Tuilier M H, Wetzel P and Gewinner G 1996 *Phys. Rev.* B **53** 1368
[12] Haderbache L, Wetzel P, Pirri C, Peruchetti J C, Bolmont D and Gewinner G 1989 *Appl. Surf. Sci.* **38** 80
[13] Kim B, Kim K J and Kang T H 1999 *Appl. Surf. Sci.* **152** 44
[14] Kim K J, Kang T H, Kim K W, Shin H J and Kim B 2000 *Appl. Surf. Sci.* **161** 268
[15] Haderbache L, Wetzel P, Pirri C, Peruchetti J C, Bolmont D and Gewinner G 1989 *Phys. Rev.* B **39** 1422
[16] Haderbache L, Wetzel P, Pirri C, Peruchetti J C, Bolmont D and Gewinner G 1990 *Thin Solid Films* **184** 365
[17] Lee E Y, Sirringhaus H and von Känel H 1994 *Phys. Rev.* B **50** 5807
[18] Weinelt M, Kutschera M, Schmidt R, Orth C, Fauster T and Rohlfing M 2005 *Appl. Phys.* A **80** 995
[19] Shumay I L, Höfer U, Reuß C, Thomann U, Wallauer W and Fauster T 1998 *Phys. Rev.* B **58** 13974
[20] Thomann U, Shumay I L, Weinelt M and Fauster T 1999 *Appl. Phys.* B **68** 531
[21] Pirri C, Peruchetti J C, Bolmont D and Gewinner G 1986 *Phys. Rev.* B **33** 4108
[22] Haderbache L, Wetzel P, Pirri C, Peruchetti J C, Bolmont D and Gewinner G 1989 *Phys. Rev.* B **39** 12704
[23] Sullivan J P, Tung R T, Eaglesham D J, Shrey F and Graham W R 1993 *J. Vac. Sci. Technol.* B **11** 1564
[24] Meyer T, Migas D, Miglio L and von Känel H 2000 *Phys. Rev. Lett.* **85** 1520
[25] Haderbache L, Wetzel P, Pirri C, Peruchetti J C, Bolmont D and Gewinner G 1990 *Rev. Phys. Appl.* **25** 869
[26] Stadler R, Podloucky R, Kresse G and Hafner J 1998 *Phys. Rev.* B **57** 4088
[27] Mattheiss L F and Hamann D R 1988 *Phys. Rev.* B **37** 10623
[28] Schattke W, Krasovskii E E, Díez Muiño R and Echenique P M 2008 *Phys. Rev.* B **78** 155314
[29] Lambrecht W R L, Christensen N E and Blöchl P 1987 *Phys. Rev.* B **36** 2493
[30] Milman V, Lee M H and Payne M C 1994 *Phys. Rev.* B **49** 16300
[31] Garreau Y, Lerch P, Jarlborg T, Walker E, Genoud P, Manuel A A and Peter M 1991 *Phys. Rev.* B **43** 14532
[32] Reuter K, de Andres P L, García-Vidal F J, Flores F and Heinz K 2000 *Appl. Surf. Sci.* **166** 103
[33] Ugur G, Soyalp F, Tütüncü H M, Duman S and Srivastava G P 2005 *J. Phys.: Condens. Matter* **17** 7127
[34] Pendry J B and Gurman S J 1975 *Surf. Sci.* **49** 87
[35] Eberhardt W and Himpsel F J 1980 *Phys. Rev.* B **21** 5572
[36] Kirchmann P S and Bovensiepen U 2008 *Phys. Rev.* B **78** 035437
[37] Ichibayashi T and Tanimura K 2007 *Phys. Rev.* B **75** 235327
[38] Weinelt M, Kutschera M, Fauster T and Rohlfing M 2004 *Phys. Rev. Lett.* **92** 126801
[39] Kentsch C, Kutschera M, Weinelt M, Fauster T and Rohlfing M 2002 *Phys. Rev.* B **65** 035323
[40] Kutschera M, Weinelt M, Rohlfing M and Fauster T 2007 *Appl. Phys.* A **88** 519
[41] Fischer R and Fauster T 1995 *Phys. Rev.* B **51** 7112
[42] Weinelt M 2002 *J. Phys.: Condens. Matter* **14** R1099
[43] Hertel T, Knoesel E, Hotzel A, Wolf M and Ertl G 1997 *J. Vac. Sci. Technol.* A **15** 1503
[44] Fauster T and Steinmann W 1995 *Photonic Probes of Surfaces* (*Electromagnetic Waves: Recent Developments in Research* vol 2) ed P Halevi (Amsterdam: North-Holland) p 347
[45] Knorren R, Bennemann K H, Burgermeister R and Aeschlimann M 2000 *Phys. Rev.* B **61** 9427
[46] Lee E Y, Sirringhaus H, Kafader U and von Känel H 1995 *Phys. Rev.* B **52** 1816
[47] Duboz J Y and Badoz P A 1991 *Phys. Rev.* B **44** 8061
[48] Rügheimer T K, Fauster T and Himpsel F J 2007 *Phys. Rev.* B **75** 121401